Check for updates

Can nitrogen input mapping from aerial imagery improve nitrous oxide emissions estimates from grazed grassland?

Juliette Maire[1,2,3,4] · Simon Gibson-Poole[1,4] · Nicholas Cowan[2] · Dominika Krol[3] ·
Cathal Somers[3] · Dave S. Reay[4] · Ute Skiba[2] · Robert M. Rees[1] · Gary J. Lanigan[3] ·
Karl G. Richards[3]

Abstract

Most nitrogen (N) lost to the environment from grazed grassland is produced as a result of N excreted by livestock, released in the form of nitrous oxide (N_2O) emissions, nitrate leaching and ammonia volatilisation. In addition to the N fertiliser applied, excreta deposited by grazing livestock constitute a heterogeneous excess of N, creating spatial hotspots of N losses. This study presents a yearlong N_2O emissions map from a typical intensively managed temperate grassland, grazed periodically by a dairy herd. The excreta deposition mapping was undertaken using high-resolution RGB images captured with a remotely piloted aircraft system combined with N_2O emissions measurements using closed statics chambers. The annual N_2O emissions were estimated to be 3.36 ± 0.30 kg N_2O–N ha^{-1} after a total N applied from fertiliser and excreta of 608 ± 40 kg N ha^{-1} yr^{-1}. Emissions of N_2O were 1.9, 3.6 and 4.4 times lower than that estimated using the default IPCC 2019, 2006 or country-specific emission factors, respectively. The spatial distribution and size of excreta deposits was non-uniform, and in each grazing period, an average of 15.1% of the field was covered by urine patches and 1.0% by dung deposits. Some areas of the field repeatedly received urine deposits, accounting for an estimated total of 2410 kg N ha^{-1}. The method reported in this study can provide better estimates of how management practices can mitigate N_2O emissions, to develop more efficient selective approaches to fertiliser application, targeted nitrification inhibitor application and improvements in the current N_2O inventory estimation.

Keywords Remote sensing · Spatial distribution map · IPCC inventory · Variable rate application · UAV

✉ Juliette Maire
juliette.maire@sruc.ac.uk

Karl G. Richards
Karl.Richards@teagasc.ie

1   Scotland's Rural College, West Mains Road, Edinburgh, UK

2   Centre for Ecology and Hydrology, Penicuik, Edinburgh, UK

3   Environmental Research Centre, Teagasc Johnstown Castle, Co. Wexford, Ireland

4   School of Geosciences, University of Edinburgh, The King's Buildings, Edinburgh, UK

Introduction

Nitrous oxide (N_2O) plays a major role in the depletion of the ozone layer (Ravishankara et al., 2009), as well as being a powerful greenhouse gas (GHG) (IPCC et al., 2013). N_2O is naturally produced in the soil, predominantly by two microbial processes; (i) nitrification, which is an aerobic process that depends on the availability of oxygen and ammonium (NH_4^+), and (ii) denitrification, an anaerobic process that depends on the availability of nitrate (NO_3^-), oxygen and carbon (C) (Davidson, 1991). N_2O emissions are enhanced by the anthropogenic supply of nitrogen (N), largely due to agricultural activities such as fertiliser application and livestock waste management. As well as N availability (e.g. fertiliser, livestock excreta, mineralising crop residues), microbial N_2O production is also dependant on soil conditions (e.g. texture, pH, and moisture content) and, weather conditions (e.g. rainfall, temperature) (Martins et al., 2017; Rowlings et al., 2015; Samad et al., 2016). These conditions can be highly spatially and temporally variable within fields and the wider environment, leading to high uncertainties in reporting of N_2O emissions from heterogeneous ecosystems such as grazed grasslands (Chadwick et al., 2018; Cowan et al., 2015; Hutchings et al., 2007; Luo et al., 2017).

The N content of the livestock excreta depends on multiple factors such as the livestock diet (percentage of crude protein), gross energy, air temperature and livestock N use efficiency (NUE) (Angelidis et al., 2019). In grazing systems, a large proportion of N ingested by livestock is returned to the soil as excreta (75% to 95%) (Van Middelaar et al., 2013). The excreta deposits become hotspots of N loss due to their high N loading in a small concentrated area, exceeding the potential of the soil and vegetation to assimilate it (Chadwick et al., 2014). The heterogeneity of the emissions at the field scale is reflected in very large variabilities associated with the national inventory of N_2O emissions. For instance, the UK GHG inventory was estimated to include over 250% uncertainty for N_2O emissions from soil (Misselbrook et al., 2011). The default emissions factor (EF) for excreta often overestimates observed pasture emissions (Bell et al., 2015; Chadwick et al., 2018) with EFs associated with urine deposition ranging from 0 to 14% (n=40) (Aarons et al., 2017; Selbie et al., 2015). N_2O emissions have been observed to have a nonlinear response to N loading and in particular cattle urinary N have high N loading rates up to 2000 kg N ha^{-1}, making them especially prone to high N_2O losses (Cai & Akiyama, 2016; Selbie et al., 2015).

Other studies have attempted to improve field scale N_2O emission measurements using eddy covariance flux tower or fast-box methods (Brümmer et al., 2017; Jones et al., 2011; Scanlon & Kiely, 2003; Voglmeier et al., 2019). However, grazed grassland has an additional challenge due to the randomly deposited excreta which makes the use of conventional up-scaling methods difficult (e.g. kriging) without a map of the precise location of the depositions (Cowan et al., 2015; Jolly et al., 2019; Levy et al., 2016). In recent years, the importance of spatial variability in N deposition from livestock has been recognised as a critical factor controlling N_2O emissions with new studies providing state-of-the-art flux measurements (De Rosa et al., 2020; Wecking et al., 2020). Currently, modelling N losses from grazed systems requires data on excreta deposition (i.e. frequency, volume, N loading, composition, their spatial distribution) (Cook & Kelliher, 2016; Snow et al., 2017). Better models will improve our understanding of N cycling from a grazed landscape and enable the location of critical source areas of N emissions so that emissions mitigation can be targeted (Betteridge et al., 2010).

In this study, small-scale plots were utilised to quantify N_2O emissions from animal excreta using static chambers, and then overall pasture emissions were estimated based on

the up-scaling of these emissions combined with excreta deposits maps. The maps were created from a Remotely Piloted Aircraft Systems (RPAS) survey before and after each grazing period, to estimate the areas where urine or dung was deposited. The method employed for this experiment uses the grass response to the N input from urine and directly assesses the dung deposits through an object-based algorithm improved from Maire et al., (2018).

The use of remote sensing and RPAS in particular is expanding across all types of farms and applications (Kim et al., 2019). The market for agricultural RPAS is therefore expected to continue growing in parallel with related technologies. Using RPAS imagery is reasonably easy to implement, gives timely results that can be integrated into existing management practices and application systems, and more importantly, is cost effective to operate (Zhang & Kovacs, 2012). Therefore, RPAS technology appears to be well placed to gain traction with the farming and advisory community with repeatable and non-invasive sampling, offering a quick and systematic way to treat and analyse the data from the images, while limiting potential human error. Moreover, their applications are spreading in many areas of agriculture, including for instance landscape prospecting and fertiliser spreading, seed planting, variable rate application of fertiliser, lime or other treatments, fertility assessment and crop yield forecasting (Florence et al., 2020; Kim et al., 2019; Lehmann et al., 2016; Mogili & Deepak, 2018; Wang et al., 2017). Remote sensing technologies such as RPAS equipped with sensors have been used to study crop and grassland systems, however, these studies have mostly been limited to individual grazing events and focussed on biomass estimation (Alvarez-Hess et al., 2021; Grüner et al., 2019; Wang et al., 2017). Nonetheless, RPAS technology is limited by the quality of the data that can be captured and field protocols need to be followed to assure the data quality as well as environmental conditions to allow stable conditions and illumination (Von Bueren et al., 2015).

The main goal of this study was to quantify and map the N input to an intensively managed dairy farm field grazed over the whole year, in the forms of fertiliser or livestock excreta to estimate their related N_2O emissions. The knowledge of the spatial pattern of the N input is a fundamental need to create variable rate application (VRA) of N fertiliser or to target nitrification inhibitor applications to the field to mitigate N_2O emissions (Balafoutis et al., 2017). Therefore, the objectives of this study were to 1) calculate EFs for cattle urine, cattle dung and, fertiliser; 2) calculate total excreta N input into the field using excreta patches mapping; 3) apply EFs to the N input map to estimate total N_2O emissions and the source partitions of these emissions; 4) compare the resulting field emissions with the results of the IPCC based calculations for the same field.

Materials and methods

Site description and grassland management

The methodology used in this study begins with the measurement of the emissions from excreta deposition and fertiliser applications and is described in Maire et al. (2020). Mapping of the excreta depositions using the RPAS surveys was then used to spatially and temporally scale the emissions from discrete grazing events to the field scale for the entire year. The experiment was conducted at an intensively managed grazed field, which formed part of the research dairy farm at Teagasc Johnstown Castle research centre, co. Wexford, Ireland (52°17′54.1" N, 6°30′01.1" W).The grassland sward mainly consisted of perennial

ryegrass (*Lolium perenne L.*). The field was managed as a rotational grazing system with a typical rotation period of about 20 days. As well as chamber flux measurements, soil and grass samples were collected during the experimentation period in an excluded experimental area within the middle of the 1.42 ha field from March 2017 to December 2017. The whole field was surveyed using a small RPAS before and after each grazing period (Figs. 1, 2). During the experiment, the intermittent grazing started in early April and finished mid-November. During this time, nine full rotations took place, corresponding to a total of 29 days grazing (stocking density of 3.4 LSU ha^{-1}, 60 dairy cows). Over the same period, the field was fertilised nine times with calcium ammonium nitrate (CAN) at a total of 261 kg of N ha^{-1}. During the grazing period, N input to the field mainly occurred in the form of N excreta and to a less extent as synthetic mineral N fertiliser.

Field N$_2$O flux measurements

As described in Maire et al. (2020), a randomised block plot experimental design was used conducted in the grazing excluded area in the centre of the field. Five replicates of (a) untreated control; (b) cattle urine; (c) CAN mineral fertiliser; and (d) cattle urine with

	Start	End	Activity	Survey images
Spring	01/03/2017		Beginning of the experiment	
	13/03/2017		Fertiliser CAN 35 kg ha^{-1}	
	31/03/2017	01/04/2017	Grazing	
	04/04/2017		RPAS survey (a)	
	10/04/2017		Fertiliser CAN 30 kg ha^{-1}	
	29/04/2017	01/05/2017	Grazing	
	02/05/2017		RPAS survey (b)	
	04/05/2017		Fertiliser CAN 30 kg	
	20/05/2017	21/05/2017	Grazing	
	23/05/2017		RPAS survey (c)	
	23/05/2017		Fertiliser CAN 30 kg ha^{-1}	
Summer	02/06/2017		RPAS survey (d)	
	06/06/2017	08/06/2017	Grazing	
	09/06/2017		RPAS survey (e)	
	14/06/2017		Fertiliser CAN 30 kg ha^{-1}	
	28/06/2017	30/06/2017	Grazing	
	01/07/2017		RPAS survey (f)	
	03/07/2017		Fertiliser CAN 30 kg ha^{-1}	
	13/07/2017		RPAS survey (g)	
	18/07/2017	19/07/2017	Grazing	
	31/07/2017		RPAS survey (h)	
	31/07/2017		Fertiliser CAN 25 kg ha^{-1}	
	16/08/2017	17/08/2017	Grazing	
	21/08/2017		RPAS survey (i)	
	25/08/2017		Fertiliser CAN 21 kg ha^{-1}	
Autumn	13/09/2017		Fertiliser CAN 30 kg ha^{-1}	
	22/09/2017	26/09/2017	Grazing	
	25/09/2017		RPAS survey (j)	
	13/11/2017		RPAS survey (k)	
	14/11/2017	16/11/2017	Grazing	
	23/11/2017		RPAS survey (l)	
	01/12/2017		End of the experiment	

Fig. 1 Timeline of the experimental field management including mineral fertiliser application events in the form of CAN and days of grazing for a herd of 60 dairy cows. Images show detailed field conditions (urine and dung patches) of the exact same spot on the ground at each RPAS survey (~4 m.^{2}) marked in surveyed chronological order with letters from (**a**) to (**l**)
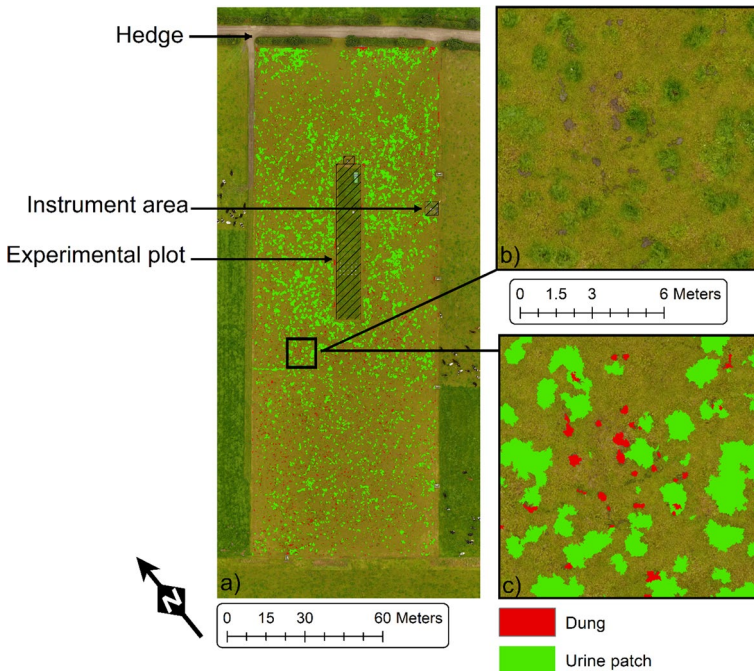
Fig. 2 **a** Entire orthomosaic of the field captured on the 21st of August 2017 showing the classified deposition of urine and dung and showing the different sections of the field (experimental plot, scientific instrument area and hedges) which were excluded from the classification; **b** A section of the original orthomosaic of (**a**), the area covered is approximately 65 m.²; **c** Classification map of the excreta deposition showing the same area as (**b**). The class "untouched" including the area where no excreta have been detected is not represented. This figure was created using Quantum GIS from the orthomosaic and the classification raster from eCognition

CAN mineral fertiliser, were applied inside static chambers and over the separate area for gas, soil and grass samples. Applications were made in spring (27/04/2017), summer (03/07/2017) and autumn (02/10/2017). Urine was collected for each season from dairy cows and stored at 5 °C prior to analysis and application. Urine N loading was measured in each season by analysing N content (Aquakem 600 discrete analyser Rigas Labs S.A) of the urine collected at the farm during milking, while dung N loading was taken from an experiment conducted in 2014 on the same farm by Krol et al. (2016) (Table 1). The N applied in the urine ranged from 573 to 671 kg N ha^{-1} (Table 1). Urine was applied in compliance with the work of Forrestal et al. (2016) where the urine patch simulation method mimics natural deposits by using a urine volume and N content similar to that of the animal. This practice allows for natural infiltration of the urine volume into the soil, replicating real conditions.

Emission factors

A mix of IPCC and experimental EFs were used in this study to account for the whole nitrogen input to the grazed grassland. The field-specific EFs of fertiliser application and urine deposition were defined in Maire et al. (2020) while the field-specific EFs allocated

Table 1 N input and calculated EFs associated with the 2017 experimental set up for CAN, urine and dung application under the different EFs hypothesis (field-specific, country-specific, IPCC 2006 and IPCC 2019 revisions)

	Spring	Summer	Autumn
Fertiliser (CAN)			
N input (kg N ha.$^{-1}$)	125	106	30
EF field-specific (%) [c]	0.31	0.07	0.72
EF country-specific (%) [a]	1.49	1.49	1.49
lPCC default 2006 EF (%)	1	1	1
lPCC default 2019 EF (%) [b]	1	1	1
Urine			
N input (kg N ha.$^{-1}$)	573	680	671
EF field-specific (%) [c]	0.33	0.28	0.82
EF country-specific (%) [a]	1.2	1.2	1.2
lPCC default 2006 EF (%)	2	2	2
lPCC default 2019 EF (%) [b]	0.4	0.4	0.4
Dung			
N input (kg N ha^{-1}).[a]	490	469	420
EF field-specific (%) [a]	0.06	0.16	0.24
EF country-specific (%)	0.31	0.31	0.31
lPCC default 2006 EF (%)	2	2	2
lPCC default 2019 EF (%) [b]	0.4	0.4	0.4

[a]Data from (Krol et al., 2016)

[b]Table 11.1 (updated) IPCC 2019 revisions GHG guidelines

[c]Data from (Maire et al., 2020)

to dung depositions were collected previously on the same farm by Krol et al., (2016). To match the fertilisation rate with surrounding grazed areas, the CAN application rates varied depending on the season (Table 1). From this experiment, EFs were calculated for the treatments applied in spring, summer, and autumn and are presented in Table 1 named as "field-specific EFs". The EFs were calculated over a 40 day period after application to ensure the comparability of the treatments between seasons (Skiba et al., 2013).

The IPCC 2019 revisions of the EF for urine and dung deposits was updated from IPCC 2006 EFs based on the work of Cai and Akiyama (2016) and 27 additional studies with a total of 461 recently measured EFs. The updated EFs for excreta deposits are disaggregated by climate (dry and wet), and are much lower than the IPCC 2006 EFs and are lower than the Irish country-specific EFs.

IPCC calculations for annual N$_2$O emissions estimation

The spatial calculations performed for this study were compared to the IPCC methodology results based on an annual account of the N$_2$O emissions from the herd of grazing dairy cows and the fertiliser applied during the year. The calculations followed the IPCC methodology published in 2006 in the IPCC guidelines for national greenhouse gas inventories (IPCC et al., 2006) but also the 2019 revisions of the IPCC guidelines (IPCC et al., 2019). In brief, in the Tier 1 approach, the amount of N applied to the field is multiplied with the EF; EF$_1$ refers to the percentage N lost as N$_2$O emissions per kg N applied in the form of synthetic nitrogen which is set to a default value of 1%; EF$_3$ refers to the N$_2$O emission

associated per N kg animal excreta applied directly to the pasture, which has a default value of 2%. The Tier 2 approach is similar to the Tier 1 approach, except it applies more defined emission factors and other parameters which are specific to the country. IPCC methodology is commonly used to quantify total emissions at a country level; however, similar approaches can be used to estimate annual emissions at a field level using Eqs. (1) and (2).

$$N_2O\,Direct = \left[n * N_{ex} * AWMS * EF_3 + N_{CAN} * EF_1 \right] * \frac{44}{28} \qquad (1)$$

$N_2O\,Direct$: annual direct N_2O emissions produced from soils from urine and dung deposition, kg N_2O yr^{-1} (per ha if divided by the total area of the field in ha).

n: number of livestock head.

N_{ex}: annual amount of urine and dung N deposited on pasture by grazing animals, kg N $yr.^{-1}$

$AWMS$: fraction of total annual nitrogen excretion that is managed in manure management system (pasture/ paddock) = ratio of annual days of grazing per year.

EF_3: emission factor for N_2O emissions from urine and dung N deposited on pasture, range and paddock by grazing animals, kg N_2O –N (kg N input).$^{-1}$

N_{CAN}: annual amount of synthetic N fertiliser applied on pasture.

EF_1: emissions factor for N_2O emissions from synthetic fertiliser kg N_2O –N (kg N input).$^{-1}$

(44/28): conversion of N_2O –N emissions to N_2O emissions

$$N_{ex} = N_{rate} * \frac{TAM}{1000} * 365 \qquad (2)$$

N_{ex}: annual amount of urine and dung N deposited on pasture by grazing animals, kg N head^{-1} yr.$^{-1}$

N_{rate}: default N excretion rate, kg N (1000 kg animal mass)$^{-1}$ day.$^{-1}$

TAM: typical animal mass kg animal.$^{-1}$

To calculate the total N excreted by the herd during the year of grazing, two approaches were used: (i) calculated using Eq. 3 from IPCC recommendations with 0.54 as N_{rate} and 600 kg as TAM which are the default revised 2019 IPCC value for west European agriculture (IPCC et al., 2019) which is equivalent to 0.320 kg of N deposited per animal per day of grazing in the form of dung and urine (Oenema et al., 2014; Velthof et al., 2015); (ii) using the default Irish-specific value for N_{ex} which is 100.9 kg head^{-1} yr.$^{-1}$ (Duffy et al., 2018). Based on the calculations above and the data in Table 1 the total emissions produced in the field during 2017 were calculated and presented in Table 2. Grass residues related emissions were not accounted for in the calculations.

Remote sensing

Aircraft, inboard sensor and image acquisition

The aircraft deployed for surveying was a small RPAS (DJI Phantom 4, Shenzhen, China) with a 1/2.3″ CMOS camera (effective pixels:12.4 M). The small RPAS followed the same flight plan for each survey conducted. The flight plan was created prior to the survey, for a flight at 35 m altitude, taking 182 pictures over the whole area with 80% forward and side overlapping. The JPEG images collected were orthorectified and turned into an

Table 2 Parameters and results of the calculations of the total N_2O-N emissions emitted from the herd of 60 dairy cows grazing a field of 1.42 ha in 2017 based on IPCC methodology (Tier 1 and Tier 2)

	Tier 1		Tier 2	
	IPCC 2006	IPCC 2019 revisions	Irish country-specific	Field-specific
n	60	60	60	60
AWMS	29/365	29/365	29/365	spring: 8 days; summer: 12 days; autumn: 9 days
N_{CAN}	261 (kg ha.⁻¹)*1.42 (ha) =370.62 kg	261 (kg ha.⁻¹)*1.42 (ha) =370.62 kg	261 (kg ha.⁻¹)*1.42 (ha) =370.62 kg	spring: 177 kg summer: 150.5 kg autumn: 42.6 kg
TAM	600	600	–	–
N_{ex} (*600/1000)*365	118.3	118.3	100.9 from (Duffy et al., 2018) Nex allocation: urine=78.4% and dung=21.6% from (Lantinga et al., 1987; Selbie et al., 2015)	100.9 from (Duffy et al., 2018) Nex allocation: urine=78.4% and dung=21.6% from (Lantinga et al., 1987; Selbie et al., 2015)
EF3	2%	0.4%	1.18% Urine 0.31% Dung	See Table 1
EF1	1%	1%	1.49%	See Table 1
Field area	1.42 ha	1.42 ha	1.42 ha	1.42 ha
Comment	–	–	–	Sum of all season results for each N source
Total N (kg yr⁻¹ ha.⁻¹)	658.2	658.2	599.7	599.7
Total N_2O (kg N_2O-N yr⁻¹ ha.⁻¹)	16.58	6.60	11.39	3.17

orthomosaic using the photogrammetric software Agisoft Photoscan (v1.2.0; Agisoft LLC, St. Petersburg, Russia), using highest image alignment options and high dense cloud settings with mild depth filtering. The red, green, blue (RGB) orthomosaic and digital surface model (DSM) were created with a resolution of 1.37 cm and 2.76 cm per pixel respectively. Twelve ground control points placed around and within the studied field were recorded using a Trimble R8S GNSS Real-Time Kinematic (RTK) GPS total station (maximum precision of 8 mm horizontally and 15 mm vertically) (Trimble Germany GmbH, 2013) and were used to improve the geolocation accuracy of the RGB orthomosaic and DSM.

Object-based classification in eCognition

Each orthomosaic was classified using the object-based image analysis (OBIA) software eCognition Developer (v9.3.1; Trimble, Munich, Germany). The goal of the classification was to detect three different classes of vegetation/terrain: (i) urine patches (i.e. visible consequences of urine deposition on grass growth, such as greener, darker and taller grass), (ii) dung deposits, (iii) untouched areas of the field (i.e. areas with no visible enhanced grass growth or dung deposit). For each survey, the entire field area was segmented into individual image objects using eCognition's multiresolution segmentation algorithm (parameters: RGB weight of 1 each; scale = 20; shape = 0.3; compactness = 0.9). Then a supervised classification was applied based on sample objects selected from areas representing each of the three classes. As for the ground control for the remote sensing imagery, a Trimble R8S GNSS RTK GPS was used to select a location in the field of urine and dung deposition in August before the RPAS survey was conducted. The GPS locations were used to create the training samples using eCognition user interface. The classification was performed using eCognitions Nearest Neighbour (NN) method (Trimble Germany GmbH, 2013). The NN method is a supervised classification that is trained by using a set of samples of different classes selected by the user, to assign membership values to all other objects. Membership values in the range 0 (no assignment) to 1 (full assignment) are assigned to each object, according to the distance in the feature space using an exponential membership function. The slope of the membership function is a combination of fuzzy function and is adjusted from the samples selected by the user, with each image object being allocated a membership value to each class (Benz et al., 2004). The closer the image object is located in the feature space to a sample of a class, the higher the membership degree to this class, with the highest membership being the class selected for each particular image object (Trimble Germany GmbH, 2013). 21 spectral and geometric attributes were considered as predictor variables for the classification (Table 5). The spectral attributes included the object's mean RGB values, brightness and skewness for each band, colour indices (Table 3) and the geometric attributes of object area, shape index, compactness and roundness.

Classification calibration and training samples

The classification training samples used to adjust the classification algorithm was selected in the segmentate image of the 21st of August survey. About 50 polygons from the segmentation for each category were selected representing less than 1% of the total field area and manually classified. The classification results were tested using 214 randomly selected samples within the survey and validated (see "Performance of the object-based classification" section for more details). To apply this algorithm to other surveys from different season, an addition of 10 to 30 manually classified samples were added and the algorithm was

Table 3 Colour indices description and references

Abbreviations	Name	Formula	References
DGR	Dark Green Index	g-r	Golzarian et al. (2012)
NDI	Normalized Difference Index	(g-r)/(g+r)	Zhang et al. (2019)
ExG	Excessive Green Index	2 g–r–b	Yang et al. (2015) and Zhang et al. (2019)
ExGR	Excessive Green Index—Excessive Red Index	ExG-(1.4*r-g)	Yang et al. (2015) and Zhang et al. (2019)
VEG	Vegetative Index	$g/(r^{0.667}*b^{0.333})$	Yang et al. (2015)
VARI (also named EVI)	Visible Atmospherically Resistant Index	(g-r)/(g+r-b)	Gitelson et al. (2002) and Zhang et al. (2019)
CIVE	Color Index of Vegetation Extraction	0.441*r-0.881*g+0.385*b+18.78745	Ponti (2013) and Yang et al. (2015)
GLI	Green Leaf Index	(2 g−b−r)/(2 g+b+r)	Zhang et al. (2019)
HSI	Hue Intensity Saturation	$\text{Tan.}^{-1}(\text{sqrt}(3)*(g\text{-}b)/[(r\text{-}g)+(r\text{-}b)])$	Chien and Tseng (2017)

readjusted using again the entire parameters selection used in this study. The re-adjustment step allowed the algorithm to be more precise for surveys where the grass growth were changed by the seasonal changes such as the grass becoming brown in autumn. The parameters selected in the re-adjustment step is presented in Table 5. Although, the accuracy reached with the NN algorithm for this study was over the suggested overall accuracy level (Ye et al., 2018), some objects were misclassified. To limit misclassification, the central experimental plot, hedges, fences and the instrument areas were removed from the classification. When shadows, bare soil and other plant species (weeds) were misclassified, further samples were added during the re-adjustment step to improve the NN classification (Alirezaie et al., 2018). Consequently, different NN classifications were applied to the surveys. A total of 12 surveys were classified, each using a separate combination of samples from the algorithm training dataset which were randomly selected for each survey date with a total of 793 samples (Table 4) and optimised set of attributes for the NN method (Table 5).

The purpose of considering surveys for detecting only dung or only urine patches was to minimise classification error by choosing the best survey available in terms of time period after grazing. Indeed, dung was more visible just after grazing when it was untouched and fresh in contrast to being dried (whiter) and dispersed by birds or animals at later time periods after deposition. Urine patches were easier to detect 10 days after grazing, as the effect on grass becomes more obvious (Dennis et al., 2011; Jolly et al., 2019).

Accuracy assessment

The eCognition version used did not offer a tool for selecting random samples for accuracy assessment, therefore the assessment for each supervised classification was completed using Quantum GIS (QGIS Development Team, 2019). For each survey date, points were generated randomly following a stratified random sampling method, where a minimum number of 50 observations are randomly placed within the classified objects of each class. The objects that were selected as the samples for the classification were not used for the accuracy assessment. All the points were then manually identified by the user before being compared with the classification from the producer (the NN classification) (Ramezan et al., 2019). User's and producer's accuracies, overall accuracy and the kappa coefficient were calculated for each survey classified. The kappa score is a statistic that is used to measure inter-rater reliability for qualitative items. It is known to be more robust measure of classification accuracy than simple percentage of agreement between the algorithm and the user as the kappa score takes into account the possibility of the agreement occurring by chance and the potential representation imbalance of the classes in the image (Ye et al., 2018). In this study, a minimum of 85% of overall accuracy was considered as an effective classification. This threshold is the traditionally accepted objective and the average accuracy reported in the literature according to Ye et al. (2018).

Annual N input and N$_2$O emissions mapping

In this study, the RPAS imagery recorded the grass stage (grass growth level and grass damaged) within the field. The grass stage coupled with a powerful trained algorithm helped to identify the location of the excreta depositions within the field. Combining the N load of one deposition associated with the average surface area by one deposition (urine or dung) from literature and field measurements, and from it, the N loading at each location

Table 4 Summary of the classification confusion matrix and accuracy results of the object-based analysis excreta deposits in each of the 12 surveys

Survey date	04-Apr[a]	02-May	23-May	02-Jun[b]	09-Jun[a]	01-Jul[a]	13-Jul[b]	31-Jul	21-Aug	25-Sep	13-Nov[b]	23-Nov	min	max	TOTAL
Accuracy (%)	96	90	89	94	91	91	89	88	91	85	89	92	**85**	**96**	–
Kappa Index (%)	92	85	83	88	77	77	71	82	86	78	75	87	**71**	**92**	–
Sample points number	52	53	53	53	53	54	50	51	214	55	53	52	–	–	**793**

Bold represent the annual minimum and annual maximum

The accuracy represents the ratio between the number of all correctly classified objects and the total number of samples. The kappa coefficient measures the proportion of agreement after removing random effects

[a]Survey used for dung only

[b]Survey used for urine patches only

Table 5 Selection of attribute features as predictor for the NN algorithm used for classifying each survey to detect urine and\or dung patches

Survey date	04-Apr[a]	02-May	23-May	02-Jun[b]	09-Jun[a]	01-Jul[a]	13-Jul[b]	31-Jul	21-Aug	25-Sep	13-Nov[b]	23-Nov	Percentage of survey using this feature
Area				x		x	x	x				x	42
Roundness				x	x					x	x	x	42
Compactness				x		x	x			x		x	42
Skewness B	x	x	x	x		x	x	x	x	x		x	83
Skewness G	x	x	x	x	x	x	x	x	x	x	x	x	100
Skewness R	x	x	x	x				x	x	x		x	67
Skewness DEM				x			x	x		x		x	42
Shape Index				x			x			x		x	33
Mean B	x	x	x						x				33
Mean G	x	x	x		x			x	x		x	x	67
Mean R		x	x	x	x	x		x	x	x	x	x	83
Hue intensity	x	x	x		x	x			x	x	x	x	75
Hue saturation	x	x	x						x	x		x	50
EXG	x	x	x		x				x	x	x		58
CIVE	x	x	x		x				x	x	x	x	67
DGR	x	x	x	x	x	x	x	x	x	x	x	x	100
VARI (also named EVI)	x	x	x			x	x	x	x	x			67
NDI		x	x	x	x	x	x	x		x	x	x	83
ExGR					x	x				x	x	x	42
VEG													0
GLI													0
[a] survey used for dung only													
[b] survey used for urine patches only													

A cross signifies that the feature has been selected as necessary after the classification optimisation. The percentage of survey using each feature represents the features most selected across the year of surveys

[a]Survey used for dung only

[b]Survey used for urine patches only

within the field for all grazing periods is established. From the resulting N load field map and EFs from measurements or literature, the total N_2O emissions of each location within the field was calculated. By summing each location emissions for all grazing period by season and by year, the total annual and seasonal emissions were estimated. A model in R software (R Development Core Team, 2019) was created for this study to map N input across the field and calculate the associated N_2O emissions for each pixel of the RPAS imagery. The model takes into account the different sources of N in grazed grassland; synthetic fertiliser as well as urine and dung deposited on pastures by grazing animals. However, the N from crop residues above or below-ground N from N-fixing crops such as clover were not taken into account and only the direct N_2O emissions were estimated (i.e. no secondary emissions from NH_3 deposition). The upscaling of the N input or emissions to the whole field for the whole year was undertaken by allocating to each pixel of each survey an amount of N input and an emission factor that was dependent on the classes assigned and the timing of the survey (Table 1). The layers were then summed by season and for the whole year using code written in the statistical data handling program R software (R Development Core Team, 2019).

Table 6 Total area covered by excreta resulting from the classification of the RPAS surveys over the year per hectare or as a percentage of the total area of the field

	Unit	Spring	Summer	Autumn	Year 2017
Percentage urine area covered	%±SD	12.7± 9.4	14.7± 4.7	19.5± 4.4	15.1± 6.1
Percentage dung area covered	%±SD	0.6± 0.3	1.2± 0.3	1.1± 0.2	1.0± 0.4
Urine N input per urination	kg N ha.$^{-1}$ per urination	202.5± 50	240.3± 50	237.1± 50	-
Dung N input per deposit	kg N ha.$^{-1}$ per deposit	490	469	420	-
Total urine N input	kg N ha.$^{-1}$	76.9± 18.95	141.1± 29.27	93.3± 19.45	310.3± 39.87
Total dung N input	kg N ha.$^{-1}$	8.2	22.0	7.7	37.9
Total fertiliser N input	kg N ha.$^{-1}$	124.8	105.8	29.9	260.5
Total N applied (urine and dung depositions, fertiliser)	kg N ha.$^{-1}$	209.8± 19.0	268.9± 29.3	130.9± 19.5	609.7± 39.9

The total N input to the field was summed over the season or whole year and presented in this table as the total value loading. The N input per deposition was calculated based on the average number of depositions per cow per day of grazing

Statistics and uncertainty calculations

Urine patches detected using the RPAS imagery can be described by i) the wetted area, where the urine is directly discharged and ii) the area directly adjacent to the wetted area where the grass has some access to the urinary N through horizontally reaching root systems and where the N can diffuse through the soil pores (Selbie et al., 2015). Indeed, the area detected by the method presented in this article is named the "effective area" (i.e. the area of grass that can be observed to be impacted by the additional N) of the urine patch which combined these two areas (Buckthought et al., 2016; Marsden et al., 2016). Accounting for the effective area and not only the wetted area is essential for accurately estimating NUE of the grass and for estimating areas of over fertilisation. Estimating the N loading on these areas was the most complex task of the model. The urine loading presented in this study (in kg N ha^{-1}) is in accordance with the literature (Hoekstra et al., 2020); however, it only considers the wetted area of the patch. The difference in extent of the wetted area and effective area has been reported to be approximately 2.83 with an average of 0.24 m^2 for the wetted area and from 0.03 to 1.1 m^2 with an average of 0.68 m^2 for the effective area (Moir et al., 2011; Selbie et al., 2015; Williams & Haynes, 1994). In the Johnstown Castle farm, urine patches have been measured with a larger area from 0.2 to 1.8 m^2 with a mean of 0.68 m^2 (Minet et al., 2016), To capture a more realistic N input to the field in the form of urinary N, the N loading for urine was divided by the wetted area ratio of 2.83 and uncertainty analysis was conducted on N loading. This analysis was undertaken using a Monte Carlo method with a range in input values from a normal distribution of the N loading (n = 10,000) with means presented in Table 6 and a standard deviation of 50. The output was used to calculate the total N input and associated emissions.

Results

Performance of the object-based classification

The urine patches and dung deposits were detected efficiently for each grazing period and allocated a hypothetical N loading depending on the season of deposition. The performance of the classification was estimated and appears to be satisfactory according to the standards published of over 85% of overall accuracy and over 70% for user's and producer's accuracy (Ramezan et al., 2019). The supervised object-based classification revealed an accuracy level minimum of 85% and maximum of 96% over all the surveys classified (n = 793, Table 4). The overall kappa number had a maximum value of 0.92 and minimum value of 0.71. Details of the producer and user accuracy for each survey are shown in the supplementary material.

In this experiment, the NN algorithm was found to be a viable algorithm to detect the excreta patches over the year. For each survey, the NN algorithm used the same group of initial features but was optimised prior to running the classification. This optimisation of the NN features for each survey meant that the final feature set selected for each classification differed for some of the surveys Table 5. These differences were implemented automatically by drawing new sample areas to more accurately distinguish patches in different states of grass growth or different states of dryness of the dung deposits.
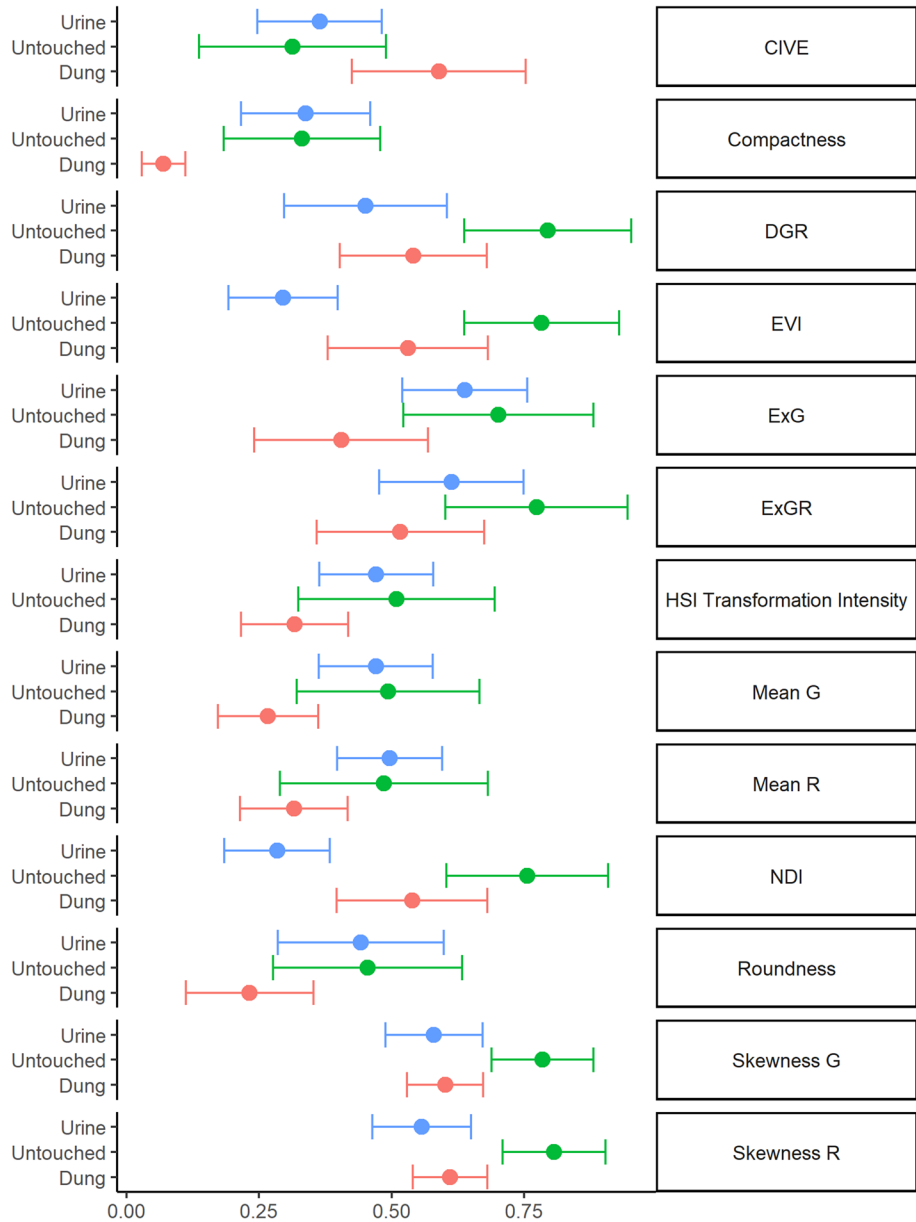
Fig. 3 Differences between classifications object features and classes. The x-axis represents the feature's values normalised between 0 and 1. Features presented are a selection of the features used for the survey on the 21/08/2017

An example of the classification results is shown in Fig. 2 along with the field features, which have been excluded from the classification (hedges, instrument area and experimental plot). For instance, the selected features from samples from the survey of the 21st of August 2017 are presented in Fig. 3. Some features such as EVI and DNI
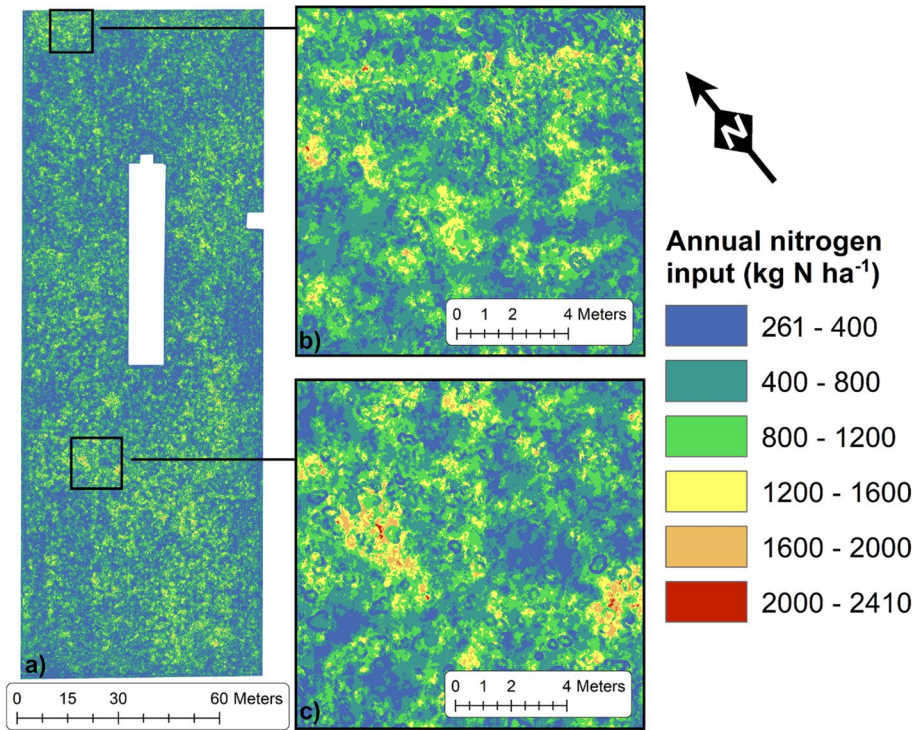
Fig. 4 **a** Resulting map of the whole field presenting the annual N from fertiliser, urine and dung deposition in kg of N ha^{-1} based on the addition of the nine grazing times of the 60 dairy cows over 2017, **b** and **c** two different sections of the annual N map showing location of high aggregation of N input. The area covered by each section is approximately 100 m.^{2}. This figure was created using Quantum GIS using the combined raster from the R model and the legend represents the range of N input rate of application which each location in the field received during the year of study

in Fig. 3 showed differences between all classes whereas some features such as CIVE, Compactness and DGR where more efficient at discerning between two classes. The classes that are more efficient at discerning between urine, dung and the untouched category are the main ones selected after NN optimisation per survey.

Total excreta coverage and nitrogen input to the field

During the typical year of grazing (April 2017 to November 2017), the average urine patches coverage for one event of 2 to 4 days (60 cows in a 1.42 ha field) was 15.1% with a maximum reached at the last grazing event of the year with 23.2%. The dung coverage was lower as expected with an average of 1.0% of the field and reached a maximum of 1.4% per grazing event (Table 6). The resulting map of total N input to the field from the excreta deposits classification and mineral fertiliser is presented in Fig. 4.

Upscaling the urine, dung and fertiliser N input to the entire field from the map resulted in a total N loading during the year of 608 ± 40 kg N ha^{-1} (Table 6). Some
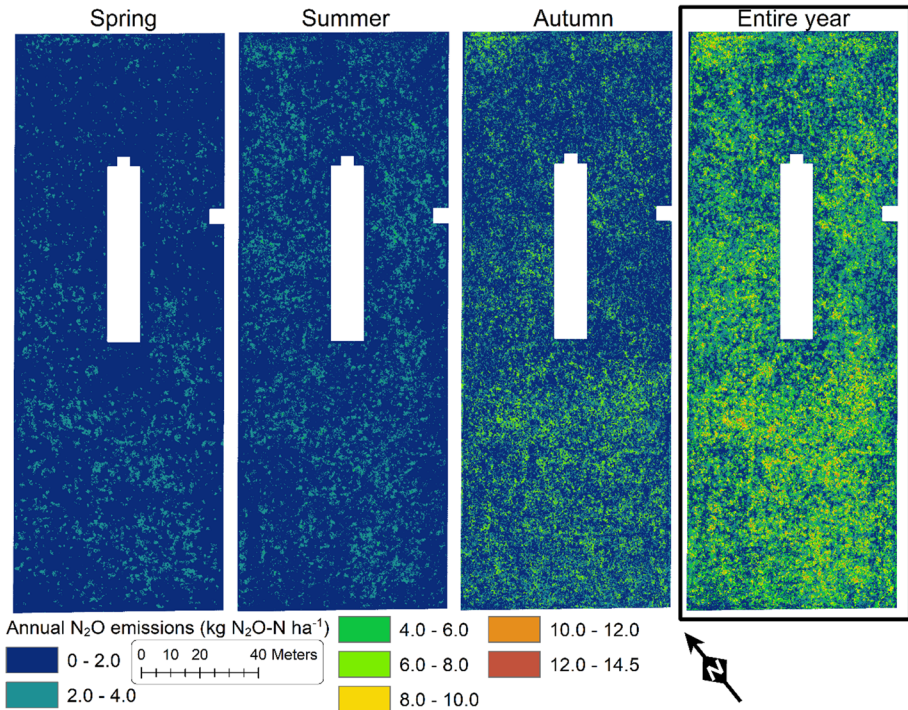
Fig. 5 Cumulative N_2O emissions maps for the entire field over the three seasons (in kg N_2O-N ha^{-1} per season) and the entire year (in kg N_2O-N ha.$^{-1}$ per year). The emissions where calculated using the field-specific EFs and the N input map and the entire year map represents the sum of the three season's value. This figure was created using Quantum GIS from the raster from the R model calculations

Table 7 Total annual N_2O emissions calculated using the RPAS imagery classification and based on the different EFs	Total N_2O emissions (urine, dung and fertiliser) (kg of N_2O-N ha.$^{-1}$)			
	Field-specific	Country-specific	IPCC 2006	IPCC 2019
Spring				
Mean	**1.01**	**4.40**	**4.62**	**2.49**
Min	0.67	3.15	2.54	2.08
Max	1.36	5.67	6.73	2.91
SD	0.10	0.36	0.59	0.12
Summer				
Mean	**0.79**	**5.24**	**6.78**	**2.69**
Min	0.24	2.86	2.81	1.89
Max	1.23	7.13	9.93	3.32
SD	0.13	0.55	0.92	0.18
Autumn				
Mean	**1.56**	**2.48**	**3.60**	**1.10**
Min	0.57	1.01	1.07	0.61
Max	2.57	3.97	6.60	1.59
SD	0.25	0.37	0.61	0.12

Mean value for the season are in bold

areas of the field were potentially touched by urine up to eight times and received a total of 2405 kg of N ha^{-1}. To test whether the excreta were deposited randomly over the field, a "Global Moran's I" spatial correlation were applied to the annual N input map after averaging the N input over a 1 m^2 scale. The N input was not randomly distributed (p-value $< 10^{-6}$) over the field with a Morgan index of 0.57 and a Z-score of 94.85.

Cumulative N$_2$O emissions from the field

From the 2017 N input map of the field, the cumulative N$_2$O emissions were estimated using field-specific EFs for the entire year and seasonally excluding winter when the field was not grazed (Fig. 5; Table 7). The spatial variability of the N$_2$O emissions at the field scale is notable with higher emissions located closer to the hedges and gates of the field due to the non-uniform distribution of the N applied.

The cumulative emissions over the three seasons were estimated to be as high as 14.40 kg N$_2$O–N ha^{-1} at some locations within the field and the higher emissions were estimated in autumn. In contrast, using the other defined EFs, summer was estimated to be the larger emissions season following by spring than autumn (Table 7). The field-specific EFs fully take account of the seasonality of the fluxes and the specificity of the year of measurement.
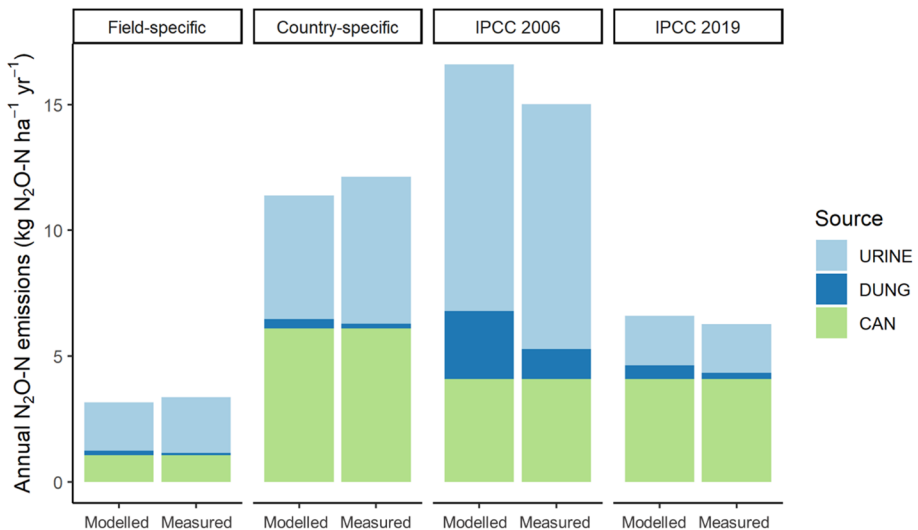
Fig. 6 Annual N$_2$O emissions partitions from different source of nitrogen (urine, dung and fertiliser CAN). The emissions have been calculated using the IPCC calculations methodology based on herd information ("Modelled") and measured using the maps of layered urine and dung deposits presented in this article ("Measured"). The calculations were performed with four EF levels: (1) field-specific measured seasonally, (2) country-specific, (3) IPCC guidelines 2006 and, (4) IPCC revisions 2019. In the "IPCC" calculations the partition between urine and dung emissions was calculated by applying the 21.6% dung vs 78.4% of urine to the N$_{ex}$

Nitrogen loading uncertainties calculations

The total annual N_2O emissions (from urine and dung deposition and fertiliser) were estimated to be 3.36 ± 0.30, 12.13 ± 0.75, 15.01 ± 1.26 and 6.28 ± 0.25 kg N_2O-N ha^{-1} yr^{-1} for the field-specific EFs, country-specific EFs, IPCC 2006 EFs and IPCC 2019 respectively. The annual N_2O emissions from the field were measured with this method with an uncertainty of 6.9% in average (Table 7). The annual N_2O emissions uncertainty includes only the urinary N loading effect as explained in "Statistics and uncertainty calculations" section. The seasonal partitions are reported in Table 7 and the N source partitions in Fig. 6.

Comparison of the IPCC methodology and the mapping results

The most commonly used method to estimate N_2O emissions from grazed grassland is to follow IPCC calculations methodology which is based on the total N excreted by animals grazing and the fertiliser N applied to the field multiplied by EFs. The results from the IPCC calculations ("Modelled") and the results from the mapping of excreta calculations ("Measured") are shown Fig. 6, along with the partition of the emissions from the different sources considered in this study. Both the "Modelled" and the "Measured" methods give similar results for the emissions from application of mineral fertiliser. In terms of excreta (urine and dung) related N_2O emissions, the modelled estimates based on mapping resulted in higher total annual emissions than the calculated results for field-specific and country-specific EFs. In contrast, map-based measured estimates were lower than the total emissions modelled for the IPCC 2006 and IPCC 2019 EFs (Fig. 6).

Discussion

Excreta deposits detection using RPAS imagery

The foundation of this study is the precision and accuracy of detecting excreta deposits in the field under variable conditions throughout the year. The choice of using a supervised classification with a NN algorithm proved to be an efficient and easy way to quickly classify the entire field with the advantages of only requiring a small number of images to give some insights into which variable or colour indices are the most useful for the classification. Moreover, the addition of only a few samples to the algorithm training set to adjust the classification efficiency for newly captured surveys can be considered as a small step for new user compared of mapping the whole field manually. Additionally, the increase number of samples added with the addition of new surveys will eventually allow the use of more automatically calibrated algorithms. This study isa step forward for a more precise, repeatable and reliable detection process compared to more subjective or manual detection methods employed in previous published research (Dennis et al., 2013; Jolly et al., 2019; Maire et al., 2018). Nonetheless, in remote sensing, other classification methods are available, such as random forest algorithms or convolution neural networks which, with a high number of input samples, can help to produce highly accurate algorithms to detect objects in images captured under diverse conditions (Thanh Noi & Kappas, 2017). These methods could integrate the entire year image collection over multiple fields to define a

unique algorithm parametrisation to enable use of this technology on a daily basis at the farm. Some object features were recurrently chosen in the NN optimisation such as Skewness G and B, DGR, NDI, Mean R, HUE intensity that can be recommended to detect urine and dung patches from images captured with a low-cost RGB camera. The results of this study indicate that RPAS could offer a new approach to the monitoring and measurement of excreta deposition by grazing livestock, but further academic and commercial research is currently developing different methods to map the urine deposits. For instance, the Spikey© is based on using electrical conductivity to map urine patches shortly after deposition, with the objective to spread a nitrification inhibitor to the area where the urine was deposited to limit the N losses with a targeted product application (Bates et al., 2015). Recently, the Spikey results from a plot experiment have been compared to thermal camera and RPAS imagery on its capacity to detect urine patches (Jolly et al., 2019). In Jolly et al. (2019), the RPAS imagery was successful in detecting all urine patches 14 days after deposition. Roten et al., (2017) used an on-board tractor system with LIDAR technology to detect taller grass patches created by the increase of grass growth after excreta deposition. A similar approach could be investigated using RPAS imagery to detect urine patches through the creation of grass height data from motion photogrammetry (Rueda-Ayala et al., 2019). To help the fast development and encourage adoption of this method, the cost related to this technology must stay low and for this reason the images, in this article, were captured with a low-cost standard RGB camera and a widely commercialised RPAS. This type of camera is provided with the purchase of most RPAS and is also commonly onboard farm machinery for obstacle avoidance or positioning (Bacco et al., 2019). Moreover, with the development of innovative farming tools, the methodology used in this study could increase the efficiency of resource use on farms such as fertiliser application. Despite the recent technical progress, the development of variable N fertiliser rate spreaders which avoid application of N fertiliser on deposited excreta or to deliver precise application of nitrification inhibitors are not yet fully commercialised (Shaw et al., 2016) but are very promising.

Nitrogen input map at the field scale

The management of the experimental field is comparable to that of a typical temperate dairy farm with rotational grazing and intensive management to optimise grass production and grass quality (Duffy et al., 2018). Fertiliser applied to the field was considered as a homogenous application over the whole area for the calculations whereas, in practice, the mineral fertiliser pellets spreader creates a spotted layer of N fertiliser. Allocating nitrogen loading to the area receiving urine, dung or fertiliser N during the entire year was challenging for the following reasons.

Firstly, the wetted area of a urine patch and the actual response of the grass may differ (Buckthought et al., 2016). The allocation of the N loading to the area detected as a urine patch was modelled with a range of possible values and divided by 2.83 to keep the ratio between effective area and wetted area (Moir et al., 2011; Selbie et al., 2015; Williams & Haynes, 1994). The urinary N loading was modelled with the summer N content which was slightly higher than the autumn N content and does not follow reported values but was in accordance with the measured urinary N content used for the N_2O fluxes measurements (Hoekstra et al., 2020; Maire et al., 2020).

Secondly, urine patch overlaps cannot simply be ignored in modelling N losses when comparing dairy systems with contrasting management practices (Romera et al., 2012).

This study considered overlapping urine patches over different periods of grazing but did not include the potential consequences of overlapping urine patches in terms of N_2O and NO_3 losses. The effects of overlapping urine deposition have been reported and modelled for N leaching (Betteridge et al., 2010; Cichota et al., 2013; Romera et al., 2012), but the effect on N_2O emissions is still understudied. The mapping undertaken in this study could be improved by the addition of urine, dung or fertiliser overlap effect as a non-linear response of the N input to the field over the year.

Thirdly, the size of the urine patch depends on the response of the grass to the N input which is a function of the soil moisture content and time from urine deposition to allow diffusion of N into the soil pores (Balvert & Shepherd, 2015; Forrestal et al., 2016; Marsden et al., 2016). Increasing soil water content has been shown to generally result in greater N_2O production and emission from urine patches (De Klein et al., 2003; Jolly et al., 2019; Van Der Weerden et al., 2014). The RPAS surveys were captured within a variable period after grazing, 3 to 30 days after grazing. Consequently, for the same N input of one urination event, the area detected as a urine patch could be different depending on the date of survey. Furthermore, the mapping of the excreta deposits facilitates the separation between N input sources and so the emissions and mitigation practices can be allocated appropriately (fertiliser or type of excreta).

Avoiding patch double-counting

Remarkably, some areas of the field received urine deposition up to 8 times over 9 grazing events, with an estimated total N input from urine, dung and fertiliser of 2409 kg N ha^{-1}. It is essential for the model to avoid double-counting of patches between grazing periods. Double-counting of dung deposits is highly unlikely as the fresh dung deposits (dark brown) are very different from the old dung deposits (dull white). To reduce the likelihood of double-counting, the RPAS imagery used to detect dung deposits were collected just after grazing. However, dung deposit can fertilise grass and grass patches can appear at the location of the dung deposits which can be misclassified as a urine patch. Though grass patches from dung deposits have previously been reported negligible (Weeda, 1967). A 15 cm buffer around freshly deposited dung (Dennis et al., 2013) from the two previous grazing events was created and subtracted from the urine patch layer. Finally, double-counting of urine patches is less likely due to the distinct difference between fresh and old urine patches during most of the year. The likelihood of this event is high when grazing is more common (i.e. in summer). Moir et al. (2011) measured double-counting of urine patches using a modelling approach. Their results showed that about less than 6.4% of the patches would overlap between grazing. The potential overestimation of the emissions from urine patches in this study corresponded to 4.2% of the total annual emissions (0.14 kg N_2O-N ha^{-1} yr^{-1}). There is a lack of knowledge on the impacts of overlapping excreta deposition on N_2O emissions and other N losses (Balvert & Shepherd, 2015; Cichota et al., 2013; Draganova et al., 2016; Voglmeier et al., 2019). Using the mapping of the excreta depositions at the field scale combined with the knowledge of the effects of overlapping depositions could have a considerable impact on the improvement of emissions estimations (Betteridge et al., 2013). This method could also be deployed to study the impact of grazing systems (i.e. strip, mob, free, marble, and rotational) on excreta deposits distribution and overlapping rate in order to help estimate their environmental impacts.

Using N input mapping to estimate cumulative N$_2$O emissions

In addition to the spatial variability due to the microorganisms, soil properties, and the spatial heterogeneity of N input across the field, N$_2$O emissions are characterised by a random temporal variability (Smith, 2017). Most studies utilised static chambers to quantify N$_2$O emissions, which are suitable for quantifying emissions on a small spatial scale but are not ideal to measure field scale emissions from heterogeneous grazing systems (Bell et al., 2015; Cowan et al., 2015; Flechard et al., 2007). Therefore, measuring cumulative N$_2$O emissions over a full grazing year at the field scale is rarely reported due to the challenging nature of the N$_2$O emissions and the lack of large-scale precise measurement instruments. The modelling and prediction of the N$_2$O emissions at the field scale is also complicated because of: (i) the heterogeneous distribution of excreta patches of high N concentration (Di & Cameron, 2012; Snow et al., 2017), (ii) excreta patches can overlap which can change the N$_2$O emission rates from urine patches (Cichota et al., 2013; Cook & Kelliher, 2016), (iii) the fields considered are often grazed many times each year, (iv) the effect of a single urination on soil can last for several months after deposition and (v) the fate of the nitrogen from excreta strongly depends on the time of deposition (Ahmed et al., 2018; Haynes & Williams, 1993), in relation to climate conditions at urination and the following weeks. The modelled emissions using the excreta maps in this study are likely to be close to the real emissions, although it is difficult to compare it to existing field measurements. Only studies deploying eddy covariance flux towers can measure at large enough scales to capture field scale emissions, but this method also has its own limitations (Cowan et al., 2020). Using the total nitrogen input to the field in the form of urine or dung estimated by the model presented in this study and the recorded days of grazing on the field per cow, it was possible to estimate the total N excreted by animal per day. It was estimated that the N deposited per day per animal to 284 g of N with 253 g of urinary N and 31 g of faeces N which is similar to the reported value of approximately 320 g of N deposited per day of grazing in the form of dung and urine (Velthof et al., 2015). The study of the spatial distribution of deposition has historically been limited due to the difficulties of efficiently mapping at the field scale (Dennis et al., 2011; Hutchings et al., 2007; Schnyder et al., 2010). This method allows a better approximation of the N input to the field and its spatial distribution than an average value determined at the global or national level (Draganova et al., 2016; Lush et al., 2018). As farm nutrient management is becoming more regulated to reduce environmental impacts and audited through modelling, assumptions made in those models should be adequate to reflect the effects of mitigation and practices.

The Irish country-specific EFs are specific to the temperate oceanic climate observed there which is characterised by high rainfall and a lack of temperature extremes. These conditions are known to enhance N$_2$O emissions from soils (Dace & Blumberga, 2016; Rowlings et al., 2015; Van Der Weerden et al., 2014) and could explain the higher EFs compared to the default revised IPCC EFs. However, 2017 was not a typical year in term of weather which could explain the low field-specific EFs. The long-term average weather data of the experimental field (measured at Rosslare weather station, < 15 km from the site) showed that 2017 was a year of lower rainfall in spring and higher rainfall in autumn and at the end of the summer (Met Éireann, 2019) compared to the LTA. On the days of application of treatments the daily mean soil moisture deficit was 32.7 mm in spring, 25.5 mm in summer, and 1.1 mm in autumn. Dry soil conditions in spring and summer were linked to low EFs for all the treatments and the wet conditions in autumn with high EFs. In this study, wetter conditions were observed during the autumn application compared to spring

and summer applications, which are in line with climate change predictions of wetter autumns and winters and drier springs and summers in the future (Nolan et al., 2017). This change in long term weather patterns suggests that if production of N_2O is to be minimised, grassland management is a key element to consider. The emissions calculated from the mapping of the N input showed that autumn season is likely to have been the higher emitting season in 2017, when using field-specific EFs. To the contrary, using the other EFs revealed the higher emitting season to be summer, when the livestock has been in the field the longest. This difference could be attributed to the fact that the approaches other than field-specific EFs, did not account for the seasonal variability of N_2O fluxes which could have led to further agreement between estimations (Wecking et al., 2020). Accounting for N_2O seasonal variability could improve the national greenhouse gas emissions inventory (Smith, 2017) and shows the potential of mitigating N_2O and manure-derived methane emissions by removing cows in response to wet soil conditions (Van Der Weerden et al., 2017). One criticism of using Emissions factors to estimate N_2O from farms is that they are designed for national inventory reporting and reflect average climatic conditions of a number of years. However in the absence of real time meteorological data (which is likely to control emissions on a daily basis) they offer a pragmatic approach to the estimation of emissions.

Spatial distribution of excreta deposition

Excreta deposits mapping in combination with precise EFs allowed us to capture data on the temporal and spatial behaviour of dairy cows. A visual assessment of these data tends to suggest spatial autocorrelation or clustering. Annual N input was not randomly distributed over the field indicating that there was aggregation of excreta patches within the field. The spatial density patterns of the excreta deposits indicated the physical properties (e.g. slope, presence of hedges or trees) of the field have an effect on the excretion behaviour in this study. However, to date, there are few published studies on excretion behaviour by grazing cattle because measurements in the field are difficult to make. Current research is however showing a non-uniform urine patch distribution, with some studies reporting that it is influenced by factors including fence line, water tank positions, field slopes and night resting areas (Auerswald & Mayer, 2010; Betteridge et al., 2010; Misselbrook et al., 2016). On the contrary, Draganova et al. (2016) related urine patch density to the duration the cows spend in each paddock instead of the physical properties of the field. In the current study, high urine and dung density were observed close to the hedge and the gates, which is the main resting area. Resting areas have been linked to location of high rates of urination and defecation (Auerswald & Mayer, 2010). During the summer, the cows were strip grazing, and some of the strips did not include this shaded and wind protected area. The RPAS imagery approach of the current study can offer new ways to model animal behaviour. Moreover, the improvement of the image classification methodology can be used in conjunction with other methods, such as ground based cameras or animal GPS collars already applied to monitor livestock behaviour (Nakano et al., 2020).

Applications of the method and perspectives

Remote sensing has been employed to create variable N rate input for crops (e.g. wheat or maize) but the scale of the heterogeneity in grazed grassland was considerably more difficult to take into account (Bacco et al., 2019; Basso et al., 2016; Corti et al., 2019). The importance of RPAS imagery or other forms of remote sensing is increasing in Precision Agriculture (PA) scope (Pallottino et al., 2018). Precision Agriculture technology adoption can be increased if the end-users (farmers) receive quantified information of the potential improvements to farm profits and positive impacts on sustainability impact (Balafoutis et al., 2017; Moral & Serrano, 2019). This study is an essential step forward a more precise accounting and detection of the excreta deposition in the grazed grassland managed to reduce GHG emissions. Variable rate (VR) spreader technology seems to be a way to reduce the GHG emissions but needs to become more precise and cheaper for farmers to purchase as well as a modification of the European rules on RPAS flying and spreading limitations. Spreader technology is advancing quickly (Bacco et al., 2019; Hijazi et al., 2014) as well as RPAS imagery (Mogili & Deepak, 2018; Mulla, 2013). VR applications could be applied to avoid spreading fertiliser on already over fertilised areas of the field due to the excreta depositions, or spreading nitrification inhibitor directly on the excreta deposits to limit the emissions from it (Bell et al., 2016; Minet et al., 2016). VR applications is executed currently by applying a prescription map which can be generated from RPAS imagery or real-time application using sensors mounted on tractors which vary the fertiliser rate depending on the data sensed (Bacco et al., 2019; Wolters et al., 2019). The carbon footprint (including N_2O emissions and direct CO_2 emissions) from the production, distribution and use of fertilisers is estimated at between 2 and 3% of the global GHG budget (Brentrup et al., 2016). Reducing inorganic N fertiliser application in grazed grassland by avoiding spreading on excreta patches could undoubtedly mitigate N_2O emissions and other N losses by better matching N supply with N demand of the grass. Finally, having a precise N input map and N_2O emissions spatial variability would offer the potential to apply different emission factors depending on the field properties such as high soil moisture, soil pH, soil type to better represent the high spatial variability of the N_2O production from the soil.

Conclusions

RPAS technologies are rapidly evolving into low-cost, easy-to-use sensor platforms that can be deployed to collect fine-scale vegetation and soil data over large areas. However, it is necessary to develop quickly effective, reliable and parsimonious methods in time for their exploitation. In this study, RPAS imagery was employed to detect excreta deposits over a dairy cow grazed field during a full year. The method demonstrated a great potential of precise mapping of the excreta depositions. However, further investigations and cross-calibrations are needed, mainly with regard to overlapping excreta depositions and more specific N_2O emission measurements. It was also demonstrated that the IPCC default EFs and Irish country specific emissions factors might have overestimated N_2O emissions during an exceptionally dry year with a wet autumn, conditions which are predicted to be more likely in future years due to climate change. Additional research could be conducted to assess the ideal time for an RPAS survey to better detect excreta patches. With

the development of GPS on-board farm machinery and image processing, it is possible to generate datasets for agricultural decision making and highly precise variable rate spreading to limit unnecessary fertiliser application, and thus limit some of the negative environmental impacts of livestock grazing. There is a significant potential in precision agriculture for combining RPAS technology with real-time data for improved agricultural management and the evaluation of mitigation practices.

Declarations

References

Aarons, S. R., Gourley, C. J. P., Mark Powell, J., & Hannah, M. C. (2017). Estimating nitrogen excretion and deposition by lactating cows in grazed dairy systems. *Soil Research, 55*, 489–499. https://doi.org/10.1071/SR17033

Ahmed, A., Sohi, R., Roohi, R., Jois, M., Raedts, P., & Aarons, S. R. (2018). Spatially and temporally variable urinary N loads deposited by lactating cows on a grazing system dairy farm. *Journal of Environmental Management, 215*(June), 166–176. https://doi.org/10.1016/j.jenvman.2018.03.046

Alirezaie, M., Langkvist, M., Sioutis, M., & Loutfi, A. (2018). A symbolic approach for explaining errors in image classification tasks. *IJCAI-ECAI-2018 Workshop*, 16–22.

Alvarez-Hess, P. S., Thomson, A. L., Karunaratne, S. B., Douglas, M. L., Wright, M. M., Heard, J. W., Jacobs, J. L., Morse-McNabb, E. M., Wales, W. J., & Auldist, M. J. (2021). Using multispectral

data from an unmanned aerial system to estimate pasture depletion during grazing. *Animal Feed Science and Technology, 275*(February), 114880. https://doi.org/10.1016/j.anifeedsci.2021.114880

Angelidis, A., Crompton, L., Misselbrook, T., Yan, T., Reynolds, C. K., & Stergiadis, S. (2019). Evaluation and prediction of nitrogen use efficiency and outputs in faeces and urine in beef cattle. *Agriculture, Ecosystems and Environment, 280*(April), 1–15. https://doi.org/10.1016/j.agee.2019.04.013

Auerswald, K., & Mayer, F. (2010). Coupling of spatial and temporal pattern of cattle excreta patches on a low intensity pasture. *Nutrient Cycling in Agroecosystems, 88*, 275–288. https://doi.org/10.1007/s10705-009-9321-4

Bacco, M., Barsocchi, P., Ferro, E., Gotta, A., & Ruggeri, M. (2019). The digitisation of agriculture: A survey of research activities on Smart farming. *Array, 3–4*(October), 100009. https://doi.org/10.1016/j.array.2019.100009

Balafoutis, A., Beck, B., Fountas, S., Vangeyte, J., Van Der Wal, T., Soto, I., Gómez-Barbero, M., Barnes, A., & Eory, V. (2017). Precision agriculture technologies positively contributing to ghg emissions mitigation, farm productivity and economics. *Sustainability (switzerland), 9*(8), 1–28. https://doi.org/10.3390/su9081339

Balvert, S., & Shepherd, M. (2015). Does size matter? The effect of urine patch size on pasture N uptake. In L. Eds. Currie (Ed.), *Moving farm systems to improved attenuation* (pp. 1–4). http://flrc.massey.ac.nz/workshops/15/Manuscripts/Paper_Balvert_2015.pdf

Basso, B., Fiorentino, C., Cammarano, D., & Schulthess, U. (2016). Variable rate nitrogen fertilizer response in wheat using remote sensing. *Precision Agriculture, 17*(2), 168–182. https://doi.org/10.1007/s11119-015-9414-9

Bates, G., Quin, B. F., & Bishop. (2015). Low-cost detection and treatment of fresh cow urine patches. In *oving farm systems to improved attenuation* (pp. 1–12). https://www.massey.ac.nz/~flrc/workshops/15/Manuscripts/Paper_Bates_2015.pdf

Bell, M. J., Cloy, J. M., Topp, C. F. E., Ball, B. C., Bagnall, A., Rees, R. M., & Chadwick, D. R. (2016). Quantifying N_2O emissions from intensive grassland production: The role of synthetic fertilizer type, application rate, timing and nitrification inhibitors. *The Journal of Agricultural Science*. https://doi.org/10.1017/S0021859615000945

Bell, M. J., Hinton, N., Cloy, J. M., Topp, C. F. E., Rees, R. M., Cardenas, L., Scott, T., Webster, C., Ashton, R. W., Whitmore, A. P., & Williams, J. R. (2015). Nitrous oxide emissions from fertilised UK arable soils: Fluxes, emission factors and mitigation. *Agriculture, Ecosystems and Environment, 212*, 134–147. https://doi.org/10.1016/j.agee.2015.07.003

Benz, U. C., Hofmann, P., Willhauck, G., Lingenfelder, I., & Heynen, M. (2004). Multi-resolution, object-oriented fuzzy analysis of remote sensing data for GIS-ready information. *ISPRS Journal of Photogrammetry and Remote Sensing, 58*(3–4), 239–258. https://doi.org/10.1016/j.isprsjprs.2003.10.002

Betteridge, K., Costall, D. A., Li, F. Y., Luo, D., & Ganesh, S. (2013). Why we need to know what and where cows are urinating – a urine sensor to improve nitrogen models. *Proceedings of the New Zealand Grassland Association 75, 75*(November), 33–38. https://www.grassland.org.nz/publications/nzgrassland_publication_2538.php

Betteridge, K., Hoogendoorn, C., Costall, D., Carter, M., & Griffiths, W. (2010). Sensors for detecting and logging spatial distribution of urine patches of grazing female sheep and cattle. *Computers and Electronics in Agriculture, 73*(1), 66–73. https://doi.org/10.1016/j.compag.2010.04.005

Brentrup, F., Hoxha, A., & Christensen, B. (2016). Carbon footprint analysis of mineral fertilizer production in Europe and other world regions. *10th International Conference on Life Cycle Assessment of Food*, (October 2016), 482–490.

Brümmer, C., Lyshede, B., Lempio, D., Delorme, J. P., Rüffer, J. J., Fuß, R., Moffat, A. M., Hurkuck, M., Ibrom, A., Ambus, P., & Flessa, H. (2017). Gas chromatography vs. quantum cascade laser-based N2O flux measurements using a novel chamber design. *Biogeosciences, 14*(6), 1365–1381.

Buckthought, L., Clough, T., Cameron, K., Di, H., & Shepherd, M. (2016). Plant N uptake in the periphery of a bovine urine patch: Determining the 'effective area.' *New Zealand Journal of Agricultural Research, 8233*(February), 1–19. https://doi.org/10.1080/00288233.2015.1134589

Cai, Y., & Akiyama, H. (2016). Nitrogen loss factors of nitrogen trace gas emissions and leaching from excreta patches in grassland ecosystems: A summary of available data. *Science of the Total Environment, 572*, 185–195. https://doi.org/10.1016/j.scitotenv.2016.07.222

Chadwick, D. R., Cardenas, L. M., Dhanoa, M. S., Donovan, N., Misselbrook, T., Williams, J. R., Thorman, R. E., McGeough, K. L., Watson, C. J., Bell, M., & Anthony, S. G. (2018). The contribution of cattle urine and dung to nitrous oxide emissions: Quantification of country specific emission factors and

implications for national inventories. *Science of the Total Environment, 635*, 607–617. https://doi.org/10.1016/j.scitotenv.2018.04.152

Chadwick, D. R., Cardenas, L., Misselbrook, T. H., Smith, K. A., Rees, R. M., Watson, C. J., McGeough, K. L., Williams, J. R., Cloy, J. M., Thorman, R. E., & Dhanoa, M. S. (2014). Optimizing chamber methods for measuring nitrous oxide emissions from plot-based agricultural experiments. *European Journal of Soil Science, 65*(2), 295–307. https://doi.org/10.1111/ejss.12117

Chien, C.-L. L., & Tseng, D. C. (2017). Color image enhancement with exact HSI color model. *International journal of innovative computing, information and control*, 7(December 2011), 6691–6710.

Cichota, R., Snow, V. O., & Vogeler, I. (2013). Modelling nitrogen leaching from overlapping urine patches. *Environmental Modelling and Software, 41*, 15–26. https://doi.org/10.1016/j.envsoft.2012.10.011

Cook, F., & Kelliher, F. (2016). Nitrous oxide emissions from grazing cattle urine patches: Bridging the gap between measurement and stakeholder requirements. *Environmental Modelling & Software, 75*, 133–152. https://doi.org/10.1016/j.envsoft.2015.10.009

Corti, M., Cavalli, D., Cabassi, G., Vigoni, A., Degano, L., & Marino Gallina, P. (2019). Application of a low-cost camera on a UAV to estimate maize nitrogen-related variables. *Precision Agriculture, 20*(4), 675–696. https://doi.org/10.1007/s11119-018-9609-y

Cowan, N., Levy, P., Maire, J., Coyle, M., Leeson, S. R., Famulari, D., Carozzi, M., Nemitz, E., & Skiba, U. (2020). An evaluation of four years of nitrous oxide fluxes after application of ammonium nitrate and urea fertilisers measured using the eddy covariance method. *Agricultural and Forest Meteorology, 280*, 107812. https://doi.org/10.1016/j.agrformet.2019.107812

Cowan, N., Norman, P., Famulari, D., Levy, P. E., Reay, D. S., & Skiba, U. M. (2015). Spatial variability and hotspots of soil N2O fluxes from intensively grazed grassland. *Biogeosciences, 12*, 1585–1596. https://doi.org/10.5194/bg-12-1585-2015

Dace, E., & Blumberga, D. (2016). How do 28 European Union member States perform in agricultural greenhouse gas emissions? It depends on what we look at: Application of the multi-criteria analysis. *Ecological Indicators, 71*, 352–358. https://doi.org/10.1016/j.ecolind.2016.07.016

Davidson, E. A. (1991). Fluxes of nitrous oxide and nitric oxide from terrestrial ecosystems. *Microbial production and consumption of greenhouse gases: Methane, nitrous oxide, and halomethanes*, 219–235.

De Klein, C. A. M., Barton, L., Sherlock, R. R., Li, Z., & Littlejohn, R. P. (2003). Estimating a nitrous oxide emission factor for animal urine from some New Zealand pastoral soils. *Australian Journal of Soil Research, 41*(3), 381–399. https://doi.org/10.1071/SR02128

De Rosa, D., Rowlings, D. W., Fulkerson, B., Scheer, C., Friedl, J., Labadz, M., & Grace, P. R. (2020). Field-scale management and environmental drivers of N2O emissions from pasture-based dairy systems. *Nutrient Cycling in Agroecosystems, 117*(3), 299–315. https://doi.org/10.1007/s10705-020-10069-7

Dennis, S. J., Moir, J. L., Cameron, K. C., Di, H. J., Hennessy, D., & Richards, K. G. (2011). Urine patch distribution under dairy grazing at three stocking rates in Ireland. *Irish Journal of Agricultural and Food Research, 50*, 149–160.

Dennis, S. J., Moir, J. L., Cameron, K. C., Edwards, G. R., & Di, H. J. (2013). Measuring excreta patch distribution in grazed pasture through low-cost image analysis. *Grass and Forage Science, 68*(3), 378–385. https://doi.org/10.1111/gfs.12000

Di, H. J., & Cameron, K. C. (2012). How does the application of different nitrification inhibitors affect nitrous oxide emissions and nitrate leaching from cow urine in grazed pastures? *Soil Use and Management, 28*(1), 54–61. https://doi.org/10.1111/j.1475-2743.2011.00373.x

Draganova, I., Yule, I., Stevenson, M., & Betteridge, K. (2016). The effects of temporal and environmental factors on the urination behaviour of dairy cows using tracking and sensor technologies. *Precision Agriculture, 17*(4), 407–420. https://doi.org/10.1007/s11119-015-9427-4

Duffy, P., Black, K., Hyde, B., Ryan, A. M., Ponzi, J., & Alam, S. (2018). *Ireland's National Inventory Report 2018*. www.epa.ie

Flechard, C. R., Ambus, P., Skiba, U., Rees, R. M., Hensen, A., van Amstel, A., Van Den Pol-Van Dasselaar, A., Soussana, J .F., Jones, M., Clifton-Brown, J., & Raschi, A. (2007). Effects of climate and management intensity on nitrous oxide emissions in grassland systems across Europe. *Agriculture, Ecosystems and Environment, 121*(1–2), 135–152. https://doi.org/10.1016/j.agee.2006.12.024

Florence, A., Revill, A., Hoad, S., Rees, Robert M., and Williams, Mathew. (2020). Predicting wheat yield using leaf and canopy properties. *Precision Agriculture* (in press)

Forrestal, P. J., Krol, D. J., Lanigan, G. J., Jahangir, M. M. R., & Richards, K. G. (2016). An evaluation of urine patch simulation methods for nitrous oxide emission measurement. *Journal of Agricultural Science, 155*(November), 1–8. https://doi.org/10.1017/S0021859616000939

Gitelson, A. A., Kaufman, Y. J., Stark, R., & Rundquist, D. (2002). Novel algorithms for remote estimation of vegetation fraction. *Remote Sensing of Environment*. https://doi.org/10.1016/S0034-4257(01)00289-9

Golzarian, M. R., Lee, M. K., & Desbiolles, J. M. A. (2012). Evaluation of color indices for improved segmentation of plant images. *Transactions of the ASABE*.

Grüner, E., Astor, T., & Wachendorf, M. (2019). Biomass prediction of heterogeneous temperate grasslands using an SfM approach based on UAV imaging. *Agronomy, 9*(2), 54. https://doi.org/10.3390/agronomy9020054

Haynes, R. J., & Williams, P. H. (1993). Nutrient cycling and soil fertility in the grazed pasture ecosystem. *Advances in Agronomy, 49*, 119–199.

Hijazi, B., Cool, S., Vangeyte, J., Mertens, K. C., Cointault, F., Paindavoine, M., & Pieters, J. G. (2014). High speed stereovision setup for position and motion estimation of fertilizer particles leaving a centrifugal spreader. *Sensors (switzerland), 14*(11), 21466–21482. https://doi.org/10.3390/s141121466

Hoekstra, N. J., Schulte, R. P. O., Forrestal, P. J., Hennessy, D., Krol, D. J., Lanigan, G. J., Müller, C., Shalloo, L., Wall, D. P., & Richards, K. G. (2020). Scenarios to limit environmental nitrogen losses from dairy expansion. *Science of the Total Environment, 707*, 134606. https://doi.org/10.1016/j.scitotenv.2019.134606

Hutchings, N. J., Olesen, J. E., Petersen, B. M., & Berntsen, J. (2007). Modelling spatial heterogeneity in grazed grassland and its effects on nitrogen cycling and greenhouse gas emissions. *Agriculture, Ecosystems and Environment, 121*(1–2), 153–163. https://doi.org/10.1016/j.agee.2006.12.009

IPCC, Gavrilova, O., Leip, A., Dong, H., MacDonald, J. D., Bravo, C. A. G. (2019). 2019 Refinement to the 2006 IPCC Guidelines for National Greenhouse Gas Inventories (Chapter 10). *IPCC Guidelines for National Greenhouse Gas Inventories*, *4*(10), 1–224. https://www.ipcc-nggip.iges.or.jp/public/2019rf/index.html

IPCC, Paustian, K., Ravindranath, N., & Van Amstel, A. (2006). *Volume 4: Agriculture, Forestry and Other Land Use (AFOLU)* (Vol. 4).

IPCC, Stocker, T. F., D. Qin, G.-K., Plattner, M., Tignor, S. K., Allen, J. (2013). Climate Change 2013: The physical science basis. *Contribution of Working Group I to the Fifth Assessment Report of the Intergovernmental Panel on Climate Change*. https://doi.org/10.1017/CBO9781107415324

Jolly, B., Saggar, S., Luo, J., Bates, G., Smith, D., Bishop, P., Berben, P., & Lindsey, S. (2019). Technologies for mapping cow urine patches: A comparison of thermal imagery, drone imagery, and soil conductivity with Spikey-R. *Nutrient Loss Mitigations for Compliance in Agriculture, 32*, 1–10.

Jones, S. K., Famulari, D., Di Marco, C. F., Nemitz, E., Skiba, U. M., Rees, R. M., & Sutton, M. A. (2011). Nitrous oxide emissions from managed grassland: A comparison of eddy covariance and static chamber measurements. *Atmospheric Measurement Techniques, 4*(10), 2179–2194. https://doi.org/10.5194/amt-4-2179-2011

Kim, J., Kim, S., Ju, C., & Son, H. I. (2019). Unmanned aerial vehicles in agriculture: A review of perspective of platform, control, and applications. *IEEE Access, 7*, 105100–105115. https://doi.org/10.1109/ACCESS.2019.2932119

Krol, D. J., Carolan, R., Minet, E., McGeough, K. L., Watson, C. J., Forrestal, P. J., Lanigan, G. J., & Richards, K. G. (2016). Improving and disaggregating N_2O emission factors for ruminant excreta on temperate pasture soils. *Science of the Total Environment, 568*(October), 327–338. https://doi.org/10.1016/j.scitotenv.2016.06.016

Lantinga, E. A., Keuning, J. A., Groenwold, J., & Deenen, P. J. A. G. (1987). Distribution of excreted nitrogen by grazing cattle and its effects on sward quality, herbage production and utilization. *Animal Manure on Grassland and Fodder Crops. Fertilizer or Waste?*, 103–117. https://doi.org/10.1007/978-94-009-3659-1_7

Lehmann, J. R. K., Münchberger, W., Knoth, C., Blodau, C., Nieberding, F., Prinz, T., Pancotto, V. A., & Kleinebecker, T. (2016). High-resolution classification of south patagonian peat bog microforms reveals potential gaps in up-scaled CH_4 fluxes by use of Unmanned Aerial System (UAS) and CIR imagery. *Remote Sensing*, *8*(3). https://doi.org/10.3390/rs8030173

Levy, P., Cowan, N., Van, M., Famulari, D., Drewer, J., & Skiba, U. (2016). NOT THIS ONE Estimation of cumulative fluxes of nitrous oxide: Uncertainty in temporal upscaling and emission factors.

Luo, J., Wyatt, J., van der Weerden, T. J., Thomas, S. M., de Klein, C. A. M., Li, Y., Rollo, M., Lindsey, S., Ledgard, S. F., Li, J., & Ding, W. (2017). Potential hotspot areas of nitrous oxide emissions from grazed pastoral dairy farm systems. In *Advances in Agronomy* (1st ed., pp. 205–268). Elsevier Inc. https://doi.org/10.1016/bs.agron.2017.05.006

Lush, L., Wilson, R. P., Holton, M. D., Hopkins, P., Marsden, K. A., Chadwick, D. R., & King, A. J. (2018). Classification of sheep urination events using accelerometers to aid improved measurements of livestock contributions to nitrous oxide emissions. *Computers and Electronics in Agriculture*, *150*(October 2017), 170–177. https://doi.org/10.1016/j.compag.2018.04.018

Maire, J., Gibson-Poole, S., Cowan, N., Reay, D. S., Richards, K. G., Skiba, U., Rees, R. M., & Lanigan, G. J. (2018). Identifying urine patches on intensively managed grassland using aerial imagery captured

from Remotely Piloted Aircraft Systems. *Frontiers in Sustainable Food Systems, 2*(April), 1–11. https://doi.org/10.3389/fsufs.2018.00010

Maire, J., Krol, D., Pasquier, D., Cowan, N., Skiba, U., Rees, R. M., Reay, D., Lanigan, G. J., & Richards, K. G. (2020). Nitrogen fertiliser interactions with urine deposit affect nitrous oxide emissions from grazed grasslands. *Agriculture, Ecosystems and Environment, 290*(3), 106784. https://doi.org/10.1016/j.agee.2019.106784

Marsden, K. A., Jones, D. L., & Chadwick, D. R. (2016). The urine patch diffusional area: An important N^{2}O source? *Soil Biology and Biochemistry*, *92*(October 2015), 161–170. https://doi.org/10.1016/j.soilbio.2015.10.011

Martins, C. S. C., Nazaries, L., Delgado-Baquerizo, M., Macdonald, C. A., Anderson, I. C., Hobbie, S. E., Venterea, R. T., Reich, P. B., & Singh, B. K. (2017). Identifying environmental drivers of greenhouse gas emissions under warming and reduced rainfall in boreal–temperate forests. *Functional Ecology, 31*(12), 2356–2368. https://doi.org/10.1111/1365-2435.12928

Met Éireann. (2019). 1981–2010 average: Ireland's National Meteorological Service. https://www.met.ie/climate-ireland/1981-2010/rosslare.html. Accessed 8 May 2019

Minet, E., Ledgard, S. F., Grant, J., Murphy, J. B., Krol, D. J., Lanigan, G. J., Lewis, E., Forrestal, P., & Richards, K. G. (2016). Mixing dicyandiamide (DCD) with supplementary feeds for cattle: An effective method to deliver a nitrification inhibitor in urine patches. *Agriculture, Ecosystems and Environment, 231*(231), 114–121. https://doi.org/10.1016/j.agee.2016.06.033

Misselbrook, T. H., Cape, J. N., Cardenas, L. M., Chadwick, D. R., Dragosits, U., Hobbs, P. J., Nemitz, E., Reis, S., Skiba, U., & Sutton, M. A. (2011). Key unknowns in estimating atmospheric emissions from UK land management. *Atmospheric Environment, 45*, 1067–1074. https://doi.org/10.1016/j.atmosenv.2010.11.014

Misselbrook, T., Fleming, H., Camp, V., Umstatter, C., Duthie, C. A., Nicoll, L., & Waterhouse, T. (2016). Automated monitoring of urination events from grazing cattle. *Agriculture, Ecosystems and Environment, 230*, 191–198. https://doi.org/10.1016/j.agee.2016.06.006

Mogili, U. R., & Deepak, B. B. V. L. (2018). Review on application of drone systems in precision agriculture. *Procedia Computer Science, 133*, 502–509. https://doi.org/10.1016/j.procs.2018.07.063

Moir, J. L., Cameron, K. C., Di, H. J., & Fertsak, U. (2011). The spatial coverage of dairy cattle urine patches in an intensively grazed pasture system. *The Journal of Agricultural Science, 149*(2011), 473–485. https://doi.org/10.1017/S0021859610001012

Moral, F. J., & Serrano, J. M. (2019). Using low-cost geophysical survey to map soil properties and delineate management zones on grazed permanent pastures. *Precision Agriculture, 20*(5), 1000–1014. https://doi.org/10.1007/s11119-018-09631-9

Mulla, D. J. (2013). Twenty five years of remote sensing in precision agriculture: Key advances and remaining knowledge gaps. *Biosystems Engineering, 114*(4), 358–371. https://doi.org/10.1016/j.biosystemseng.2012.08.009

Nakano, T., Bavuudorj, G., Iijima, Y., & Ito, T. Y. (2020). Quantitative evaluation of grazing effect on nomadically grazed grassland ecosystems by using time-lapse cameras. *Agriculture, Ecosystems & Environment*, *287*(September 2019), 106685. https://doi.org/10.1016/j.agee.2019.106685

Nolan, P., O'Sullivan, J., & McGrath, R. (2017). Impacts of climate change on mid-twenty-first-century rainfall in Ireland: A high-resolution regional climate model ensemble approach. *International Journal of Climatology, 37*(12), 4347–4363. https://doi.org/10.1002/joc.5091

Oenema, O., Sebek, L., Kros, H., Lesschen, J. P., Krimpen, M. van, Bikker, P., van Vuuren, & Velthof, G. (2014). Methodological studies in the field of agro-environmental indicators. Lot 1 excretion factors. Task 5, (February), 1–42.

Pallottino, F., Biocca, M., Nardi, P., Figorilli, S., Menesatti, P., & Costa, C. (2018). Science mapping approach to analyze the research evolution on precision agriculture: World EU and Italian Situation. *Precision Agriculture, 19*(6), 1011–1026. https://doi.org/10.1007/s11119-018-9569-2

Ponti, M. P. (2013). Segmentation of low-cost remote sensing images combining vegetation indices and mean shift. *IEEE Geoscience and Remote Sensing Letters, 10*(1), 67–70. https://doi.org/10.1109/LGRS.2012.2193113

QGIS Development team, O. S. G. F. (2019). QGIS Geographic Information System.

R Development Core Team. (2019). R: a language and environment for statistical computing. Vienna, Austria. (Version 3.2.5 2016-04-14).

Ramezan, C., Warner, T., & Maxwell, A. (2019). Evaluation of sampling and cross-validation tuning strategies for regional-scale machine learning classification. *Remote Sensing, 11*(2), 185. https://doi.org/10.3390/rs11020185

Ravishankara, A. R., Daniel, J. S., & Portmann, R. W. (2009). Nitrous oxide (N_2O): The dominant ozone-depleting substance emitted in the 21st century. *Science, 326*, 123–125. https://doi.org/10.1126/science.1176985

Romera, A. J., Levy, G., Beukes, P. C., Clark, D. A., & Glassey, C. B. (2012). A urine patch framework to simulate nitrogen leaching on New Zealand dairy farms. *Nutrient Cycling in Agroecosystems, 92*(3), 329–346. https://doi.org/10.1007/s10705-012-9493-1

Roten, R. L., Fourie, J., Owens, J. L., Trethewey, J. A. K., Ekanayake, D. C., Werner, A., Irie, K., Hagedorn, M., & Cameron, K. C. (2017). Urine patch detection using LiDAR technology to improve nitrogen use efficiency in grazed pastures. *Computers and Electronics in Agriculture, 135*, 128–133. https://doi.org/10.1016/j.compag.2017.02.006

Rowlings, D. W., Grace, P. R., Scheer, C., & Liu, S. (2015). Rainfall variability drives interannual variation in N_2O emissions from a humid, subtropical pasture. *Science of the Total Environment, 512–513*, 8–18. https://doi.org/10.1016/j.scitotenv.2015.01.011

Rueda-Ayala, V. P., Peña, J. M., Höglind, M., Bengochea-Guevara, J. M., & Andújar, D. (2019). Comparing UAV-based technologies and RGB-D reconstruction methods for plant height and biomass monitoring on grass ley. *Sensors (switzerland), 19*(3), 1–17. https://doi.org/10.3390/s19030535

Samad, M. D. S. S., Biswas, A., Bakken, L. R., Clough, T. J., de Klein, C. A. M. M., Richards, K. G., Lanigan, G. J., & Morales, S. E. (2016). Phylogenetic and functional potential links pH and N_2O emissions in pasture soils. *Scientific Reports, 6*, 35990. https://doi.org/10.1038/srep35990

Scanlon, T. M., & Kiely, G. (2003). Ecosystem-scale measurements of nitrous oxide fluxes for an intensely grazed, fertilized grassland. *Geophysical Research Letters, 30*(16), 2–5. https://doi.org/10.1029/2003GL017454

Schnyder, H., Locher, F., & Auerswald, K. (2010). Nutrient redistribution by grazing cattle drives patterns of topsoil N and P stocks in a low-input pasture ecosystem. *Nutrient Cycling in Agroecosystems, 88*(2), 183–195. https://doi.org/10.1007/s10705-009-9334-z

Selbie, B., Buckthought, L. E., & Shepherd, M. A. (2015). The challenge of the urine patch for managing nitrogen in grazed pasture systems. *Advances in Agronomy, 129*, 229–292. https://doi.org/10.1016/bs.agron.2014.09.004

Shaw, R., Lark, R. M., Williams, A. P., Chadwick, D. R., & Jones, D. L. (2016). Characterising the within-field scale spatial variation of nitrogen in a grassland soil to inform the efficient design of in-situ nitrogen sensor networks for precision agriculture. *Agriculture, Ecosystems and Environment, 230*, 294–306. https://doi.org/10.1016/j.agee.2016.06.004

Skiba, U., Jones, S. K., Drewer, J., Helfter, C., Anderson, M., Dinsmore, K., McKenzie, R., Nemitz, E., & Sutton, M. A. (2013). Comparison of soil greenhouse gas fluxes from extensive and intensive grazing in a temperate maritime climate. *Biogeosciences, 10*(2), 1231–1241. https://doi.org/10.5194/bg-10-1231-2013

Smith, K. A. (2017). Changing views of nitrous oxide emissions from agricultural soil: Key controlling processes and assessment at different spatial scales. *European Journal of Soil Science, 12*, 137–155. https://doi.org/10.1111/ejss.12409

Snow, V. O., Cichota, R., McAuliffe, R. J., Hutchings, N. J., & Vejlin, J. (2017). Increasing the spatial scale of process-based agricultural systems models by representing heterogeneity: The case of urine patches in grazed pastures. *Environmental Modelling and Software, 90*, 89–106. https://doi.org/10.1016/j.envsoft.2017.01.005

Thanh Noi, P., & Kappas, M. (2017). Comparison of random forest, k-nearest neighbor, and support vector machine classifiers for land cover classification using sentinel-2 imagery. *Sensors, 18*(2), 18. https://doi.org/10.3390/s18010018

Trimble Germany GmbH. (2013). User Guide - eCognition ® Developer. *Trimble eCognition Developer for Windows operating system*, (March), 256. http://www.ecognition.com

Van Der Weerden, T. J., Laurenson, S., Vogeler, I., Beukes, P. C., Thomas, S. M., Rees, R. M., Topp, C. F. E., Lanigan, G., & De Klein, C. A. M. (2017). Mitigating nitrous oxide and manure-derived methane emissions by removing cows in response to wet soil conditions. *Agricultural Systems, 156*(May), 126–138. https://doi.org/10.1016/j.agsy.2017.06.010

Van Der Weerden, T. J., Manderson, A., Kelliher, F. M., & de Klein, C. A. M. M. (2014). Spatial and temporal nitrous oxide emissions from dairy cattle urine deposited onto grazed pastures across New Zealand based on soil water balance modelling. *Agriculture, Ecosystems and Environment, 189*, 92–100. https://doi.org/10.1016/j.agee.2014.03.018

Van Middelaar, C. E., Berentsen, P. B. M., Dijkstra, J., & De Boer, I. J. M. (2013). Evaluation of a feeding strategy to reduce greenhouse gas emissions from dairy farming: The level of analysis matters. *Agricultural Systems, 121*, 9–22. https://doi.org/10.1016/j.agsy.2013.05.009

Velthof, G. L., Hou, Y., & Oenema, O. (2015). Nitrogen excretion factors of livestock in the European Union: A review. *Journal of the Science of Food and Agriculture, 95*(15), 3004–3014. https://doi.org/10.1002/jsfa.7248

Voglmeier, K., Six, J., Jocher, M., & Ammann, C. (2019). Grazing related nitrous oxide emissions: From patch scale to field scale. *Biogeosciences Discussions, 16*, 1685–1703. https://doi.org/10.5194/bg-2018-435

Von Bueren, S. K., Burkart, A., Hueni, A., Rascher, U., Tuohy, M. P., & Yule, I. J. (2015). Deploying four optical UAV-based sensors over grassland: Challenges and limitations. *Biogeosciences, 12*(1), 163–175. https://doi.org/10.5194/bg-12-163-2015

Wang, D., Xin, X., Shao, Q., Brolly, M., Zhu, Z., & Chen, J. (2017). Modeling aboveground biomass in Hulunber grassland ecosystem by using unmanned aerial vehicle discrete lidar. *Sensors, 17*(180), 1–19. https://doi.org/10.3390/s17010180

Wecking, A. R., Wall, A. M., Liáng, L. L., Lindsey, S. B., Luo, J., Campbell, D. I., & Schipper, L. A. (2020). Reconciling annual nitrous oxide emissions of an intensively grazed dairy pasture determined by eddy covariance and emission factors. *Agriculture, Ecosystems and Environment, 287*(2019), 106646. https://doi.org/10.1016/j.agee.2019.106646

Weeda, W. C. (1967). The effect of cattle dung patches on pasture growth, botanical composition, and pasture utilisation. *New Zealand Journal of Agricultural Research, 10*(1), 150–159. https://doi.org/10.1080/00288233.1967.10423087

Williams, R. H., & Haynes, R. J. (1994). Comparison of initial wetting pattern, nutrient concentrations in soil solution and the fate of 15N-labelled urine in sheep and cattle urine patch areas of pasture soil. *Plant and Soil, 162*, 49–59.

Wolters, S., Söderström, M., Piikki, K., & Stenberg, M. (2019). Near-real time winter wheat N uptake from a combination of proximal and remote optical measurements: how to refine Sentinel-2 satellite images for use in a precision agriculture decision support system. In *Precision agriculture '19* (pp. 1001–1007). The Netherlands: Wageningen Academic Publishers.

Yang, W., Wang, S., Zhao, X., Zhang, J., & Feng, J. (2015). Greenness identification based on HSV decision tree. *Information Processing in Agriculture, 2*(3–4), 149–160. https://doi.org/10.1016/j.inpa.2015.07.003

Ye, S., Pontius, R. G., & Rakshit, R. (2018). A review of accuracy assessment for object-based image analysis: From per-pixel to per-polygon approaches. *ISPRS Journal of Photogrammetry and Remote Sensing, 141*(July), 137–147. https://doi.org/10.1016/j.isprsjprs.2018.04.002

Zhang, C., & Kovacs, J.M. (2012). The application of small unmanned aerial systems for precision agriculture: A review. *Precision Agriculture, 13*(6), 693–712. https://doi.org/10.1007/s11119-012-9274-5

Zhang, J., Virk, S., Porter, W., Kenworthy, K., Sullivan, D., & Schwartz, B. (2019). Applications of Unmanned Aerial Vehicle Based Imagery in Turfgrass Field Trials. *Frontiers in Plant Science*. https://doi.org/10.3389/fpls.2019.00279